Mon. Not. R. Astron. Soc. **000**, 1–5 (2005) Printed 27 July 2018 (MN LATEX style file v2.2)

Formation of a counter-rotating stellar population in the Large Magellanic Cloud: a Magellanic triplet system?

B. Armstrong[1⋆], and K. Bekki[1]
[1] *International Centre for Radio Astronomy Research/The University of Western Australia, M468, 35 Stirling Hwy, Crawley, WA, 6009*

Accepted, Received 2005 February 20; in original form

ABSTRACT
The Large Magellanic Cloud is observed to have a counter-rotating stellar population in its disc, which has not been reproduced in previous simulations of the Magellanic system. We propose a new scenario in which the origin of this counter-rotating stellar population is the result of a minor retrograde merger with another dwarf galaxy more than 3 Gyr ago, and investigate this scenario using our hydrodynamical simulations. Our simulations show that such merging can result in a counter-rotating stellar component, and a co-rotating gaseous component. We show that this counter-rotating population would not be radially concentrated, but found throughout the Large Magellanic Cloud. The thin disc of the Large Magellanic Cloud is thickened by the merging. We suggest that the Magellanic Clouds were originally a triplet system containing this companion galaxy. We then discuss previous observations of the Magellanic Clouds in the context of a triplet dwarf system, and discuss how such a merger could occur.

Key words: Magellanic Clouds – galaxies: interactions – galaxies: star formation – galaxies: stellar content

1 INTRODUCTION

The Magellanic Clouds are an invaluable source for learning about how galaxy interactions can affect the star formation and chemical evolution of galaxies. We have come to understand that many of their features, such as the Magellanic Stream (Mathewson, Cleary &, Murray 1974), must have arisen as a result of interactions between the Magellanic Clouds (Besla et al. 2010). One of the more curious features of the Large Magellanic Cloud (LMC) is the presence of a kinematically-distinct population of AGB stars with metallicities closer to that of the Small Magellanic Cloud (SMC) (Olsen et al. 2011). Olsen et al. (2011) found that the line-of-sight velocities of these stars were such that they were either counter-rotating in a similarly inclined plane as the LMC, or were co-rotating at an inclination of $54^\circ \pm 2^\circ$ relative to the LMC. Because their kinematics are linked to the HI arms E and B (Stavely-Smith et al. 2003), Olsen et al. (2011) suggested that these stars originated in the SMC, before travelling into the LMC along these infalling HI arms. This population represented ∼5% of the stars sampled by Olsen et al. (2011), which they argued indicated that ∼5% of the stars in the LMC were part of this counter-rotating population.

Previous models have failed to explain how such a population could have come to exist. While simulations have successfully reproduced unique features of the LMC-SMC binary system, such as the Magellanic Stream (e.g. Diaz & Bekki 2012), this has yet to be done for the counter-rotating population. The existence of the Magellanic Stream and Bridge suggests a prograde interaction for the SMC, but numerical simulations suggest that counter-rotating stars would require retrograde motion (Friedli 1996). Additionally, while the total mass of the SMC has not been estimated precisely (Bekki & Stanimirović 2009), an LMC-SMC mass ratio of $\leqslant 0.1$ would require the SMC to accrete 50% of its stars to reach the expected 5% of the LMC's stars. This is highly unlikely.

Since the last LMC-SMC interaction ∼0.2 Gyr ago cannot explain the mass of counter-rotating stars in the LMC (Bekki & Chiba 2007), other physical processes need to be considered. As Olsen et al. (2011) suggested, there may be no counter-rotating stars, and the apparent counter-rotation due to the inclination of the stellar disc. However, this idea is not consistent with Subramaniam & Prabhu (2005), who found additional evidence of counter-rotating stars within the LMC core. If the stars are counter-rotating, but are not a result of an LMC-SMC interaction, then these stars might originate from another dwarf galaxy that had merged with the LMC. This could mean that the Magellanic Clouds were originally a triplet dwarf system.

The purpose of this paper is to investigate the origin of

⋆ E-mail: benjamin.armstrong@icrar.org

Table 1. Description of the basic parameter values for the simulated galaxies in M1 as represented by N-body models.

Model		$M_{\rm dm}$	$M_{\rm s}$	$M_{\rm g}$	R_s [a]	R_0	Spin [b]
M1	LMC	$1.0\times10^{11}{\rm M}_\odot$	$18\times10^{8}{\rm M}_\odot$	$12\times10^{8}{\rm M}_\odot$	5.5 kpc	1.1 kpc	r
	Companion	0.1	1.8	1.2	1.8	0.35	r
M2	LMC	1.0	12	6	5.5	3.3	r
	Companion	0.1	2.4	0.6	1.8	1.0	r
M3	LMC	1.0	18	12	5.5	1.1	r
	Companion	0.1	1.8	1.2	1.8	0.35	p
M4	LMC	1.0	18	12	5.5	1.1	p
	Companion	0.1	1.8	1.2	1.8	0.35	r
M5	LMC	1.0	18	12	5.5	1.1	p
	Companion	0.1	1.8	1.2	1.8	0.35	p

[a] $R_s = R_g$
[b] The direction of the rotation relative to the orbit, where p and r indicate prograde and retrograde motion, respectively.

the apparent counter-rotating population in the LMC based on a simulation of a dwarf-LMC merging event 3–5 Gyr ago, well before the Magellanic Stream formed. Although it will have a strong impact on the results, we do not model the SMC in our simulations. Our focus is on determining whether a retrograde merger could create a counter-rotating population, rather than on creating a definitive representation of the Magellanic system ∼5 Gyr ago.

2 SIMULATION

We investigate the stellar velocities of the LMC and a hypothetical merging dwarf galaxy. To simulate the time-evolution of the LMC-companion interaction, we use our GPU-based chemodynamical simulation code (Bekki 2013, 2015). Both galaxies are assumed to consist of a dark matter halo, a stellar disc, a stellar bulge, and a gaseous disc. The total masses of dark matter halo, stellar disc, gas disc, and bulge are denoted as $M_{\rm h}$, $M_{\rm s}$, $M_{\rm g}$, and $M_{\rm b}$, respectively. We adopt the density distribution of the NFW halo (Navarro, Frenk & White 1996) as suggested from cold dark matter (CDM) simulations and the c-parameter ($c = r_{\rm vir}/r_{\rm s}$, where $r_{\rm vir}$ is the virial radius of a dark matter halo) and $r_{\rm vir}$ are chosen appropriately for a given dark halo mass ($M_{\rm dm}$) by using the $c - M_{\rm h}$ relation predicted by cosmological simulations (Neto et al. 2007). The basic parameter values for the LMC and companion are summarized in Table 1.

The radial (R) and vertical (Z) density profiles of the stellar disc are assumed to be proportional to $\exp(-R/R_0)$ with a model-dependent scale length (R_0)and to ${\rm sech}^2(Z/Z_0)$ with scale length $Z_0 = 0.04R_{\rm s}$, respectively. The gas disc with a size $R_{\rm g} = R_{\rm s}$ has a vertical scale length of $0.02R_{\rm g}$, but the radial scale length depends on the model. In M1, M3, & M4, the radial scale length is $R_0 = 0.2R_{\rm s}$, while in M2 it is $R_0 = 0.6R_{\rm s}$ The rotational velocity and initial radial and azimuthal velocity dispersions are assigned with Toomre's parameter $Q = 1.5$, and the vertical velocity dispersion is set to be half the radial velocity dispersion at a given radius.

The total number of particles used to represent the LMC and the companion is $N = 1.1\times10^6$. The softening length is assumed to be the same between old stellar, gaseous, and new stellar particles. The gravitational softening length for the dark ($\epsilon_{\rm dm}$) and baryonic components ($\epsilon_{\rm s}$) of our models are are 674 pc and 502 pc, respectively.

We assume gas particles can be converted into 'new stars' if (i) the total mass density of a gas particle ($\rho_{\rm g}$) exceeds a threshold gas density for star formation ($\rho_{\rm th}$), which we set to be $\rho_{\rm th} = 10{\rm cm}^{-3}$, (ii) the local dynamical time-scale is shorter than the sound crossing time (mimicking the Jeans instability), and (iii) the local velocity field is consistent with gravitational collapse (i.e., $\nabla\cdot\mathbf{v} < 0$). We adopt the Kennicutt–Schmidt law (SFR $\propto \rho_{\rm g}^{\alpha_{\rm sf}}$, where $\rho_{\rm g}$ is the gas density, and the power-law slope is $\alpha_{\rm sf} = 1.5$; Kennicutt 1998).

A detailed look at the models for the H_2 formation on dust grains, supernovae (SNe) feedback, metal and dust enrichment, and the dust are given in Bekki (2013). Therefore, we will only briefly mention these. Our code can account for both H_2 formation on dust grains and H_2 dissociation by far ultra-violet (FUV) radiation self-consistently. Using the spectral energy densities around each gas particle, it can derive the molecular gas fraction for each particle, and so determine the gas consumption rate by star formation (SF). We assume that 90% of the SN feedback energy increases thermal energy, while the remaining 10% increases the random motion. The code handles chemical enrichment from SF, and metal ejection from SNIa, II and AGB-stars self-consistently. We account for the time-delay between the onset of SF and the formation of SNe and AGB-stars. We adopt the nucleosynthesis yields of SNIa and II from Tsujimoto et al. (1995) and AGB stars from van den Hoek & Groenewegen (1997) Dust grows through accretion of metals onto dust grains, and are destroyed by SN blast waves. These processes are parameterized by growth and destruction time-scales, which are set to $\tau_{\rm g} = 0.25$ Gyr and $\tau_{\rm d} = 0.5$ Gyr.

The spin axes of the LMC and the companion are specified by the two angles θ_i and ϕ_i (in units of degrees), where $i = 1$ and 2 represent the LMC and the companion, respectively, θ is the angle between the z axis and the vector of the angular momentum of a disc, and ϕ is the azimuthal angle measured from x axis to the projection of the angular momentum vector of a disc on the xy plane.

We investigate models with the following orbital config-

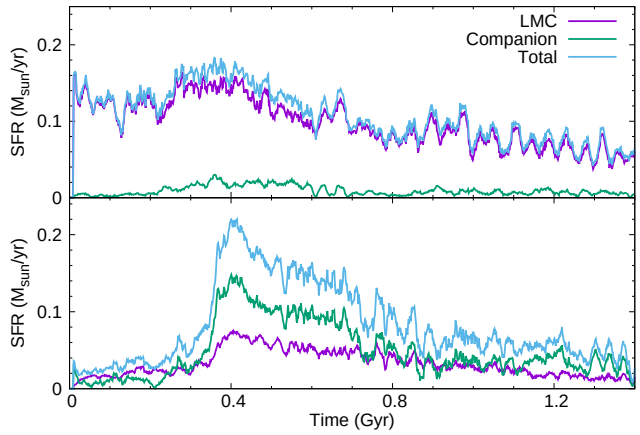

Figure 1. Top: A 15-point moving average of the SFR in the LMC, the companion, and the total (LMC + companion) for B1, a retrograde-retrograde interaction between the LMC and companion. Bottom: A 15-point moving average of the SFR in the LMC, the companion, and the total for B2, which is designed to have a lower initial LMC SFR.

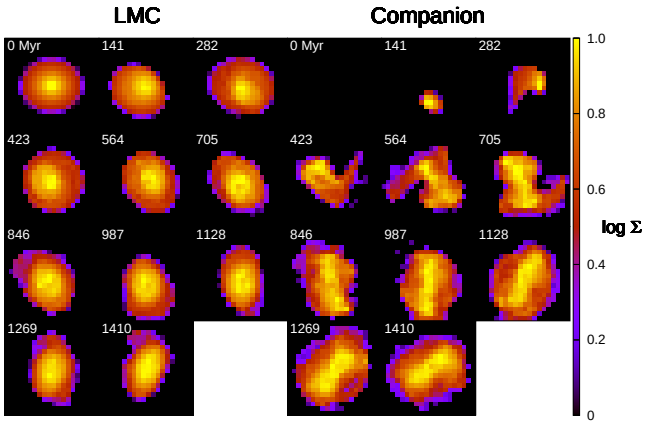

Figure 2. Surface density evolution of the stellar component in M1 throughout 1.4 Gyr of simulation on the XY-plane for both the LMC and the companion. The density is normalised between 0 and 1 for each individual plot for ease of comparison and to make small differences stand out.

uration: $\theta_1 = 45^\circ$ and -135°, $\theta_2 = 0^\circ$ and 180°, $\phi_1 = 30^\circ$ and $\phi_2 = 0^\circ$, where θ_1, ϕ_1 represent LMC and θ_2, ϕ_2 represent the SMC, $m_2 = 0.1$, $R_\mathrm{i} = 52.5$kpc, and $r_\mathrm{p} = 5.5$kpc. The differences between the models are detailed in Table 1. In the spin column, p indicates prograde motion, in which the galaxy rotates about its axis in the same direction as it orbits the other galaxy. ($\theta_1 = 45^\circ$, $\theta_2 = 0^\circ$), and r indicates retrograde motion, in which the direction of the galaxy's rotation is different to the direction of it's orbit ($\theta_1 = -135^\circ$, $\theta_2 = 180^\circ$). M1 is the fiducial model, and has a retrograde-retrograde interaction. In M2, we investigate a model designed for less star formation. M3, M4, & M5 investigate different orbital configurations.

3 RESULTS

Fig. 1 depicts the star formation rate (SFR) between the LMC and its companion over the course of the simulation. The top panel shows M1, a retrograde-retrograde interaction between the LMC and the companion, while the bottom panel shows M2, which is constructed to have a lower SFR than M1. We do this because observations from Harris & Zaritsky (2009) showed the LMC to have a very low SFR prior to 3 Gyr ago. A 15-point moving average is put through the SFR. This is done to prevent momentary fluctuations from masking the effects of the interaction, while still allowing us to observe broad changes in the SFR.

The SFR of the LMC initially starts off relatively consistently. At 0.25–0.3 Gyr, the LMC and companion merge, and we see a burst of star formation in both the LMC and the companion. The increase in SFR is similar between the models for the LMC, rising 0.11–0.15M$_\odot$/yr and 0.03–0.07M$_\odot$/yr in M1 and M2, respectively. The companion, however, sees a dramatic difference. Where in M1 it increases 0.0–0.02M$_\odot$/yr, in M2 we instead see 0.02–0.14M$_\odot$/yr. This bursty period lasts for ∼350 Myr, though this is less well defined for the LMC. After this period, the SFR slowly declines. Since our simulation treats the galaxies as exponential discs, they initially have a high central density, which may lead to the SFR of the LMC in M1 being overestimated at the beginning of the simulation. Because the initial SFR is so low, this effect on the companion and on the LMC in M2 is negligible.

We then looked at the surface densities and line-of-sight (LOS) velocities of stellar particles within a $17.5 \times 17.5 \times 17.5$ kpc cube centred on the LMC, relative to the motion of the LMC along each axis. We then divide the data into a 20×20 mesh, and take the average values within each cell. In Fig. 2, we show the surface density evolution of the stellar discs of the LMC and companion in the XY-plane throughout 1.4 Gyr of simulation. Each individual plot is normalised between 0 and 1 to highlight the differences in distributions between the LMC and the companion, and to make small variations more noticeable. In Fig. 3 and Fig. 4, we show the LOS velocities of both the stellar and gaseous components of each galaxy at the final time-step, relative to the galaxy itself. We do this along each axis for both galaxies. We examine velocities between -100 and 100 km/s only, to make small variations more distinct. The initial velocity gradient is due to the parameters of the simulation ($\theta = 45^\circ$). Over the first ∼800 Myr, the companion stars travel through the LMC, changing from a small exponential disc to a heavily disrupted and scattered collection of stars, with different parts travelling at very different speeds.

From this point onwards, the companion stars settle down into the LMC. After adopting a more disc-like structure, the companion stars form a 'bar' (Fig. 2). The companion stars are less centrally concentrated than those of the LMC. There is a clear separation between positive and negative relative velocities in the XZ- and YZ-plane (Fig. 3). The XY-plane has a less well defined divide, but there is still a clear direction of rotation. In all planes, the companion stars are counter-rotating with the LMC stars. The LMC undergoes significant precession over the interaction, and by the final time-step has gone from being edge-on to primarily facing the XZ-plane. There is already evidence of the LMC having undergone precession in the past (see van

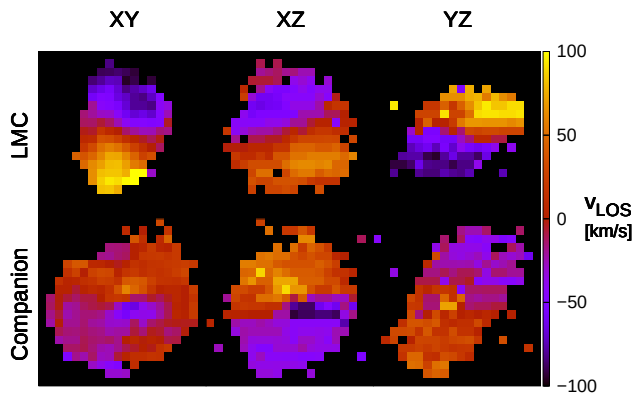

Figure 3. Relative LOS velocity of the stellar component in M1 after 1.4 Gyr along each axis for both the LMC and the companion. The minimum and maximum velocities are set to be -100 and 100 km/s to show the contours more clearly.

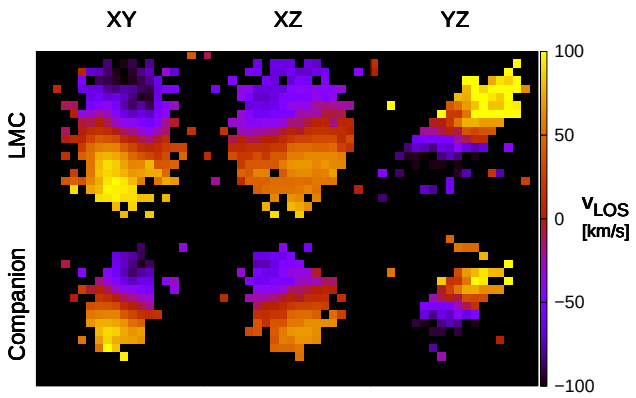

Figure 4. Relative LOS velocity of the gaseous component in M1 after 1.4 Gyr along each axis for both the LMC and the companion. The minimum and maximum velocities are set to be -100 and 100 km/s to show the contours more clearly.

der Marel et al. 2002, and references within), which might be an indication of such a merger having occurred.

The initially sharp exponential disc of the LMC seems to have been disrupted by the interaction, resulting in the thin LMC disc being thickened. Comparing the two galaxies, the companion's stars tend to be moving slower than their LMC counterparts. There is also a small region at the galaxy's core where the companion stars are moving the fastest, though not to the speed of the LMC stars. This is apparent in all planes for both M1 and M2. This is not seen in the LMC, where the stars along the rim of the disc are faster. Interestingly, far from being confined to parts of the LMC, the companion stars are more widely distributed than the LMC stars along each plane.

Compared to the old stars that existed before the merger, the distribution of the gas and the new stars born from that gas differs greatly (Fig. 4). Despite the retrograde-retrograde interaction, the gas from the companion starts co-rotating with the gas in the LMC from the second time-step onwards. This is unsurprising, the gas from the LMC and companion can directly interact and exchange energy with each other, whereas the stars cannot. It then continues to co-rotate as the LMC precesses over the interaction. While the companion stars are more widely distributed than their LMC counterparts, the gas from the companion is far more centrally concentrated. The new stars created during the simulation are also more centrally concentrated than the old stars in both the LMC and the companion, but the degree to which they co-rotate is lessened. They still do co-rotate, but since the velocity of the star is effectively 'locked-in' from the gas it formed from, there is more variation in the possible velocities at any one point.

In M3, M4, & M5, we examine the effects of different orbital configurations. We see counter-rotating stars in M3, but not in M4 or M5. The direction of the LMC's motion is what controls whether counter-rotating stars will be present. This also determines if the LMC will undergo significant precession or not. However, a retrograde companion causes the disc to be thickened more than a prograde companion.

4 DISCUSSION AND CONCLUSIONS

An interaction between the LMC and the SMC was proposed by Olsen et al. (2011) as a possible origin of the kinematically-distinct AGB-stars in the LMC, but such a feature has not been reproduced in prior simulations. Therefore, we propose that this took place with a different dwarf galaxy, which merged with the LMC to create a counter-rotating population of stars. This is supported by the clear counter-rotating stellar component present in our simulation results. There is existing evidence supporting the counter-rotation proposal over the inclined co-rotating disc that Olsen et al. (2011) also suggest. Subramaniam & Prabhu (2005) found that, out to a radius of 3°, there is a distinct counter-rotating region in the core of the LMC. Importantly, we do not find any counter-rotation in the gaseous component, which is consistent with the lack of detection of any gas counter-rotation in observations.

Since the kinematically-distinct population is thought to make up ∼5% of the LMC's stars, the mass of the merged companion must have been small relative to the LMC. To make up 5% of the LMC's stellar content, the companion would need to have a total mass of approximately $5 \times 10^{10} M_{\odot}$. The counter-rotating population in our simulations is spread throughout the LMC (Fig. 2). This is similar to the observations of Olsen et al. (2011), with the notable absence of a sparse distribution in the LMC bar. We can compare this with other products in galaxy interactions in the LMC. The HI in the LMC consists of two features, the L- and D-components, with different velocities (Luks & Rohlfs 1992). This is thought to be the result of tidal stripping between the LMC and SMC (Fukui et al. 2017). However, the distribution of the L-component is highly asymmetric, and the gas co-rotates with the LMC. Since the L-component has yet to reach equilibrium with the D-component but is still co-rotating, it must have been accreted from a co-rotating source, such as the SMC. This, along with the clear differences in spatial distributions, suggests that the formation of the L-component and the kinematically distinct population were due to different types of interactions, which is consistent with our explanation.

We can place constraints on when this merger must have occurred by understanding the star formation history (SFH) of the LMC. One of the unusual properties of the LMC is that the age distribution of its globular clusters shows a distinct gap, stretching from 3 to 13 Gyr ago (Bekki et al. 2004). The LMC's SFH depicts this "age gap" as a long, quiescent epoch, which lasted until SF resumed ∼5 Gyr ago (Harris & Zaritsky 2009; Rubele et al. 2012; Monteagudo et al. 2018). Since the merger must have occurred long enough ago so as to leave no obvious trace, but cannot have occurred during the quiescent period, the LMC-companion merger was likely responsible for the starburst in the LMC 3–5 Gyr ago. Because observed features of the Magellanic system, such as the Magellanic stream, are thought to have been created during the most recent LMC-SMC interaction, the LMC-companion merger should not have an impact on their formation, and should be able to co-exist with models reproducing these features.

Interestingly, both Harris & Zaritsky (2009) and Rubele et al. (2012) note the SFH of the SMC coincides with the LMC up until the age gap, but lacks an equivalent quiescent period. They both interpret this as being a result of LMC-SMC-Galaxy interactions. However, recent results suggest that the LMC and SMC are undergoing their first interaction with the Galaxy (Besla et al. 2007). If the ongoing cluster formation in the SMC is due to past interactions with the companion, then the SMC may contain evidence of these interactions. However, the companion does not necessarily need to have interacted with the SMC and could have just had a much closer orbit to the LMC than the SMC did, which would explain why the SMC was not affected by the LMC-companion merger.

While this merger may have occurred 3–5 Gyr ago, we do not see any direct evidence in the Magellanic system that it took place. However, this does not mean that such features did not exist in the past. Because of the large mass difference between the LMC and the companion, it is possible that the LMC would not have been greatly disturbed by the interaction, and been able to retain most of it's gas. We might also expect to find evidence imprinted in the LMC, however because of ongoing SMC interactions the features may be interpreted as having a different origin. An example of this might be the LMC's thick disc, which Bekki & Chiba (2005) claimed was formed by strong interactions with the SMC and Galaxy over the last 9 Gyr. While originally modelled as a thin exponential disc, the LMC in our simulations is disrupted by the interaction, resulting in a thickened disc forming. This is consistent with previous observations of the shape of the LMC (van der Marel 2001, 2002).

If the Magellanic Clouds had previously existed as part of a larger group of dwarf galaxies, then the likelihood of the LMC undergoing a merger with a companion is increased. An unusual feature of the dwarf galaxies in the Local Group is that many of them, including the Magellanic Clouds, are orbiting the Milky Way in roughly the same plane (Kroupa, Theis & Boily 2004). One of the suggested formation models of this feature is that the dwarf galaxies were accreted as a group, rather than individually (D'Onghia & Lake 2008). This has also been proposed as an origin of the common diffuse dark matter halo between the Magellanic Clouds (Bekki 2008), which is used to tie together proper-motion measurements of the SMC (Kallivayalil et al. 2006) with tidal interaction models featuring the Magellanic Stream (e.g. Diaz & Bekki 2012). These findings are consistent with and support our proposed scenario. If a metal-poor, gas-rich dwarf indeed merged with the LMC more than 3 Gyr ago, then the chemical evolution and the star formation history of the LMC after the merger event could have been significantly influenced by the rapid supply of such metal-poor gas. Fossil records of such a gas infall event might be imprinted on the chemical abundances of the LMC.

ACKNOWLEDGEMENTS

We thank the anonymous referee for their comments and suggestions that have helped improve this paper.

5 REFERENCES

Bekki K., 2013, MNRAS, 436, 2254
Bekki K., 2015, MNRAS, 449, 1625
Bekki K., Chiba M., 2005, MNRAS, 356, 680
Bekki K., Chiba M., 2007, PASA, 24, 21
Bekki K., Stanimirović S., 2009, MNRAS, 395, 342
Bekki K., Couch W. J., Beasley M. A., Forbes D. A., Chiba M., Da Costa G. S., 2004, ApJ, 610, L93
Besla G., Kallivayalil N., Hernquist L., Robertson B., Cox T. J., van der Marel R. P., Alcock C., 2007, ApJ, 668, 949
Besla G., Kallivayalil N., Hernquist L., van der Marel R. P., Cox T. J., Kereš D., 2010, ApJ, 721, L97
Diaz J. D., Bekki K., 2012, ApJ, 750, 36
D'Onghia E., Lake G., 2008, ApJ, 686, L61
Friedli D., 1996, A&A, 312, 761
Fukui Y., Tsuge K., Sano H., Bekki K., Yozin C., Tachihara K., Inoue T., 2017, PASJ, 69, L5
Harris J., Zaritsky D., 2009, AJ, 138, 1243
Kennicutt R. C. Jr., 1998, ApJ, 498, 541
Kroupa P., Theis C., Boily C. M., 2004, A&A, 431, 517
Luks T., Rohlfs K., 1992, A&A, 263, 41L
Mathewson D. S., Cleary M. N., Murray J. D., 2974, 190, 291
Monteagudo L., Gallart C., Monelli M., Bernard E. J., Stetson P. B., 2018, MNRAS, 473, L16
Navarro J. F., Frenk C. S., White S. D. M., 1996, ApJ, 462, 563
Neto A. F. et al., 2007, MNRAS, 381, 1450
Olsen K. A. G., Zaritsky D., Blum R. D., Boyer M. L., Gordon K. D., 2011, ApJ, 737, 29
Rubele et al. 2012, A&A, 537, A106
Stavely-Smith L., Kim S., Calabretta M. R., Haynes R. F., Kesteven M. J., 2003, MNRAS, 339, 87
Subramaniam A., Prabhu T. P., 2005, ApJ, 625, L47
Tsujimoto T., Nomoto K., Yoshii Y., Hashimoto M., Yanagida S., Thielemann F.-K., 1995, MNRAS, 277, 945
van den Hoek L. B., Groenewegen M. A. T., A&AS, 318, 231
van der Marel R. P., AJ, 2001, 122, 1827
van der Marel R. P., Alves D. R., Hardy, E., Suntzeff N. B., AJ, 2002, 124, 2639